Journal of Rock Mechanics and Tunnelling Technology (JRMTT)
29 (1) 2023 pp 49-66

Available online at www.isrmtt.com

Correlating Textural Parameters with Joint Roughness for Himalayan Schist and Gneissic rocks

Som Nath[1,2], Ashok K. Singh[3], Jagadish Kundu[4], H. K. Verma[2], R. D. Dwivedi[3], N. Rai[1]*

[1]*Department of Earth Sciences, Indian Institute of Technology, Roorkee, Uttarakhand, India*
[2]*CSIR-Central Institute of Mining and Fuel Research, Research Centre Bilaspur (CG), India*
[3]*CSIR-Central Institute of Mining and Fuel Research, Research Centre Roorkee (UK) India*
[4]*Department of Earth Sciences, Sapienza University of Rome, Pale Aldo Moro, Italy*

**Email: ashokkumar@cimfr.nic.in*

ABSTRACT

The shear strength characteristics of jointed rock masses are interrelated to the roughness of joint surfaces. These joint surfaces are characterized by mineral grains and their textural arrangements such as orientation, size, shape, degree of grain linking, and relative quantities of grains and matrix in a rock which varies accordingly. Textural Coefficient (TC), a dimensionless quantitative measure, is often used to quantify the intrinsic textural characteristics of rocks. The Joint roughness coefficient (JRC) is a metric that is frequently used to characterize rock mass roughness in the field that inherently controls the inter-block shear strength of jointed rock masses. This parameter has significant importance in the indirect assessment of rock mass strength to be used in a variety of rock engineering projects and has a direct association with the inherent textural parameters. Therefore, in the present work, we have made observations on the Himalayan schist and gneissic lithologies to quantify the potential control of textural characteristics (TC) on joint roughness (JRC). The JRC for studied rock types were measured in field and then statistically derived from the 2D surface profiles using the root means square of the first derivative of the profile outline (Z_2). The TC values for studied rock types were estimated using microphotographs of respective joint surfaces. The statistical analyses suggest two groups of data correlation controlled by a threshold TC value of 1.1. Both the groups showed a strong linear correlation between JRC and TC for the studied lithologies signifying the control of textural characteristics on joint roughness. As a result of the study, empirical equations have been proposed to quantify the JRC from Z_2 as well as using TC.

Keywords: Textural coefficient; Joint roughness coefficient; Statistical correlations; Himalayan lithology.

1. INTRODUCTION

Joint is a discontinuity plane of natural origin with no visible displacement (ISRM, 1978). The profile of the joint surface exhibits an arrangement of crests and troughs called asperities. These asperities make the joint surface rough and are quantified by their inclination with the joint plane. The shear strength characteristics of rock masses strongly depend on the joint parameters such as its attitude, wall compressive strength, surface waviness or undulation, aperture, infilling etc. of the discontinuity surface which ultimately governs the deformational behaviour of rock masses (Goodman and Shi, 1985). Along with the joint compressive strength, the basic or residual friction angle of joint surfaces control the inter-block shear behaviour and associated stability which is also governed by the roughness of the joint surfaces (Bhasin and Hoeg, 1998). The joint roughness is inherently associated with the mineral and grain arrangement of rock and the contact area of the surface (Schneider, 1976). These irregularities are called roughness of the rocks and can be defined as the degree of surface unevenness. The roughness of jointed rock mass massively affects the mechanical property and deformability of the rock masses and has enormous implications in various domains of rock engineering projects as well as in landslide modelling (Gupta et al., 2023; Singh et al., 2021; Barton, 2013; Prasad et al., 2013; Barton et al., 1974). Barton and Choubey (1977) have introduced a coefficient called Joint Roughness Coefficient (JRC) to quantitatively represent the roughness of joint surfaces. Depending on the unevenness, the JRC value ranges from 0 for the smoothest to 20 for the roughest with an interval of 2 (Barton and Choubey, 1977). Shearing resistance during rock block movement, in general, the joint surface arises two parameters, one is from frictional resistance and the second component is the geometric irregularities of the sliding surfaces (Barton, 1971; Patton et al., 1966). Barton-Bandis' model (Barton et al., 1985; Bandis et al., 1981; Barton, 1973), one of the most used constitutive strength criteria to model jointed rock mass, also uses JRC as a parameter as shown in Equation 1.

$$\tau = \sigma \tan\left(JRC \log\left({}^{JCS}/_{\sigma}\right) + \phi_b\right) \quad (1)$$

where τ is the peak shear strength of the rock joint, σ is the normal stress, JCS is joint compressive strength in MPa, and ϕ_b is the basic friction angle of joints. Grain size is an effective parameter in determining JRC thereby shear behaviour of rock joints, so correlating JRC with microscopic parameters shall be proved informative to assess the lithological control on joint roughness (Kabeya and Legge, 1997).

Generally, the JRC of a particular 2D rock surface profile is accessed by visual estimation and comparison with the standard profile proposed by Barton and Choubey (1977). This method effectively minimizes the inherent subjectivity involved in roughness quantification in the field. However, with advancement in computing and instrumentation, researchers across the globe have tried to quantify the JRC more precisely considering micro-scale roughness features of the joint profile. Therefore, literature introduced quantitative measurement techniques for the JRC determination from 2D surface profiles (Wang et al., 2017; Tatone and Grasselli, 2010; Yang et al., 2001; Kabeya and Legge, 1997; Yu and Vayssade, 1991; Tse and Cruden, 1979). Several methods and empirical relations have been formulated for the assessment of JRC by correlating with the parameters such as roughness profile index, profile elongation, the ultimate slope of the profile, arithmetical mean deviation roughness index of the profile, rootmean square roughness index of the profile etc. (Table 1).

Since the surface roughness of rock joints depends on the mineralogical properties and their inter-grain relationship, however as per the authors' best knowledge, no study is available in literature correlating these two vital parameters. Therefore, in the present work, an attempt has been made to correlate the JRC of natural joints with the textural properties for varieties of Himalayan Gneissic and Schistose rocks. The textural coefficient was evaluated by quantifying the elementary parameters of grains and their interrelationship using petrographic analysis. To estimate the JRC, the root means-square of the first derivative of the profile outline (Z_2) models proposed by Tse and Cruden (1979) has been utilized which established the regression correlations between JRC and Z_2. This technique is quite frequently used by many researchers successfully (Li and Huang, 2015; Li and Zhang, 2015). Subsequently, statistical analyses have been carried out to observe the correlation between JRC and textural indices.

2. LITERATURE REVIEW

Joint roughness is a major factor that influences the shear strength and deformability characteristics of jointed rock masses. Usually, determining the roughness of a discontinuity surface and providing a numerical value is essential and require considerable effort in rock engineering projects. Though the methods and guidelines of roughness measurement of discontinuity surface are well formulated (ISRM, 1978), other quantitative methods have evolved. Some of these methods include laser scanning, 3D imaging using photogrammetry, rock joint roughness based on Terrestrial Laser Scanner, and Image Analysis (Abolfazli and Fahimifar, 2020; Tatone and Grasselli, 2013; Bae et al., 2011; Baker et al., 2008; Rahman et al., 2006; Kulatilake et al., 1997). The nature of the data produced by these methods and the restrictions on their usage should be properly understood since they offer data that are fundamentally different from conventionally established methods. Additionally, these methods are generally laboratory-based and need time and skill to process the data. In contrast, an on-site quick estimation of joint roughness data is requisite in rock engineering projects as rock mass classification systems used in these projects incorporate joint roughness as one of the important parameters to provide weightage or rating in the categorization of the rock masses. So, the conventional roughness estimation through a roughness profilometer is quite handy and reliable for an on-site assessment. Conventionally, JRC is measured through visual comparison with the standard 2D surface profile that involved inherent subjectivity provided experience in practice. Therefore, convenient and simple empirical models based on statistical methods are frequently used to obtain the roughness parameter. Some important empirical relations along with important parameters that are frequently used in JRC estimation are listed in Table 1. The readers can refer the literature as indicated in Table 1 for more details on JRC estimation using various surface roughness parameters.

Table 1- Some important surface roughness parameters given in literature

Unified Term	Definition	Calculation	References
R_P	Roughness Profile Index: It is the ratio of true length of the roughness profile (L_t) to projected length of the profile i.e., the length along abscissa	$\mathrm{Rp} = L_t/\mathrm{L}$ $L_t = \sum_{i=1}^{N=1} \sqrt{(x_{i+1}-x_i)^2 + \frac{(y_{i+1}-y_i)^2}{(x_{i+1}-x_i)}}$ $L = \sum_{i=1}^{N=1} (x_{i+1}-x_i)$	Yu and Vayssade (1991); Tatone and Grasselli (2010)
δ	Profile Elongation Index: The ratio of difference of true length of the roughness profile (L_t) to projected length of the profile (L).	$\delta = (L_t - L)/L$	Yu and Vayssade (2010); Maerz et al. (1990)
δ_L	Profile Elongation Rate: Percentage	$\delta_{L`} = \delta \times 100$	Wang (1982)

	difference between the true length and the projected length of a profile		
λ	The ultimate slope of the profile: The ratio of maximum height of profile to projected length of profile, along the abscissa.	R_Z/L	Barton and de Quadros (1997)
R_a	Arithmetical mean deviation roughness index of the profile, mm	$R_a = 1/L \int_{x=0}^{x=l} \lvert Y \rvert dx = 1/L \sum_{i=1}^{N=1} Y_i \lVert \Delta s$	Tse and Cruden (1979)
R_q	Root mean square roughness index of the profile, mm	$R_q = \left[1/M \int_{x=0}^{x=M} y^2\, dx\right]^2 = \left[1/M \sum_{i=1}^{N=1} {y_i}^2\, \Delta s\right]^{1/2}$	Tse and Cruden (1979)
Z_2	Root mean square of the first derivative of the profile outline	$Z_2 = \left[\int_{x=0}^{x=L} (dy/dx)^2\, dx\right]^2 = \left[1/L \sum_{i=1}^{N=1} \frac{(y_{i+1} - y_i)^2}{(x_{i+1} - x_i)}\right]^{1/2}$	Tse and Cruden (1979); Yu and Vayssade (1991); Yang et al. (2001); Tatone and Grasselli (2010)
M_S	Mean square value roughness index	$M_s = \left[1/M \int_{x=0}^{x=M} y^2\, dx\right] = \left[1/M \sum_{i=1}^{N=1} {y_i}^2\, \Delta s\right]$	Tse and Cruden (1979)
σ_i	The standard deviation of the angle *i*	$\sigma_i = \tan^{-1}\left[1/L \int_{x=0}^{x=L} (\frac{dy}{dx} - \tan i_{ave})^2 dx\right]^{1/2}$ $i_{ave} = 1/L \int_{x=0}^{x=L} \tan^{-1}(\frac{dy}{dx}) dx$	Yu and Vayssade (1991)
SF	Structure-function, mm^2	$SF = 1/L \int_{x=0}^{x=L} [f(x + dx) - f(x)]^2\, dx = 1/L \Sigma (y_{i+1} - y_i)^2 \Delta x$	Tse and Cruden(1979); Yu and Vayssade (1991) Yang et al. (2001)

Notations: *dx- increment of x of the profile; dy- increment of y of the profile; N- number of evenly spaced sampling points; M- number of sample intervals; L- projected length of the profile, the length along abscissa;* L_t*- true length of the profile; Δs- sampling interval;* R_z*- maximum height of the profile, equal to the vertical distance between the highest peak and lowest valley.*

Among the listed parameters for roughness estimation, Z_2 is widely used for its reliability and a good correlation coefficient with the observed value. Table 2 provides the various empirical correlations proposed in the literature for the calculation of JRC using Z_2. Therefore, the best correlation proposed by Tse & Cruden (1979) has been considered for the quantitative assessment of JRC in the present study. The equations proposed by Tse & Cruden (1979) are formulated to numerically characterize the surface roughness measured on the ten profiles presented by Barton and Choubey (1977) on a sampling interval of 1.27 mm. These correlations are the three variants for JRC assessment using various functions of Z_2 such as logarithmic and arctan of Z_2. Yu and Vayssade (1991) suggested three correlations based on the sampling interval of 0.25, 0.5 and 1 mm. Similarly, Tatone and Grasselli (2010) power correlation to estimate JRC with the sampling interval of 0.5 mm and 1 mm.

Table 2- Some of the empirical correlations proposed in the literature for JRC estimation using Z_2

No.	Equations	R^2	Sampling Interval (mm)	References
1	$JRC = 32.2 + 32.47\log(Z_2)$	0.986	1.27	Tse and Cruden (1979)
2	$JRC = -4.41 + 64.46\,Z_2$	0.968	1.27	
3	$JRC = -5.05 + 1.20\,tan^{-1}(Z_2)$	0.973	1.27	
4	$JRC = 32.69 + 32.98\log(Z_2)$	0.993	0.5	Yang et al. (2001)
5	$JRC = 60.32Z_2 - 4.51$	0.968	0.25	Yu and Vayssade (1991)
6	$JRC = 61.79Z_2 - 3.47$	0.973	0.5	
7	$JRC = 64.22Z_2 - 2.31$	0.983	1.0	
8	$JRC = 51.85(Z_2)^{0.60} - 10.37$	-	0.5	Tatone and Grasselli (2010)
9	$JRC = 55.85(Z_2)^{0.74} - 6.10$	-	1.0	

3. STUDY AREA AND FIELD INVESTIGATION

The goal of the site selection procedure is to collect and analyse enough information to demonstrate how the mineral grains parameter and the mineralogy of rocks may influence the roughness profile. Since the goal of the current work is to establish a connection between JRC and textural coefficients, the availability of multiple lithologies has been considered in the site selection approach. The location was chosen so that we could get variations in joint roughness profile data for various rock types. So, on that basis, the study area was selected in the portion of lower and higher Himalayan topographies along about 40 km stretch of National Highway (NH)-5 in Himachal Pradesh, India. The area is extended from Jhakri of Shimla district to Nigulsari of Kinnaur district of Himachal Pradesh (Fig. 1).

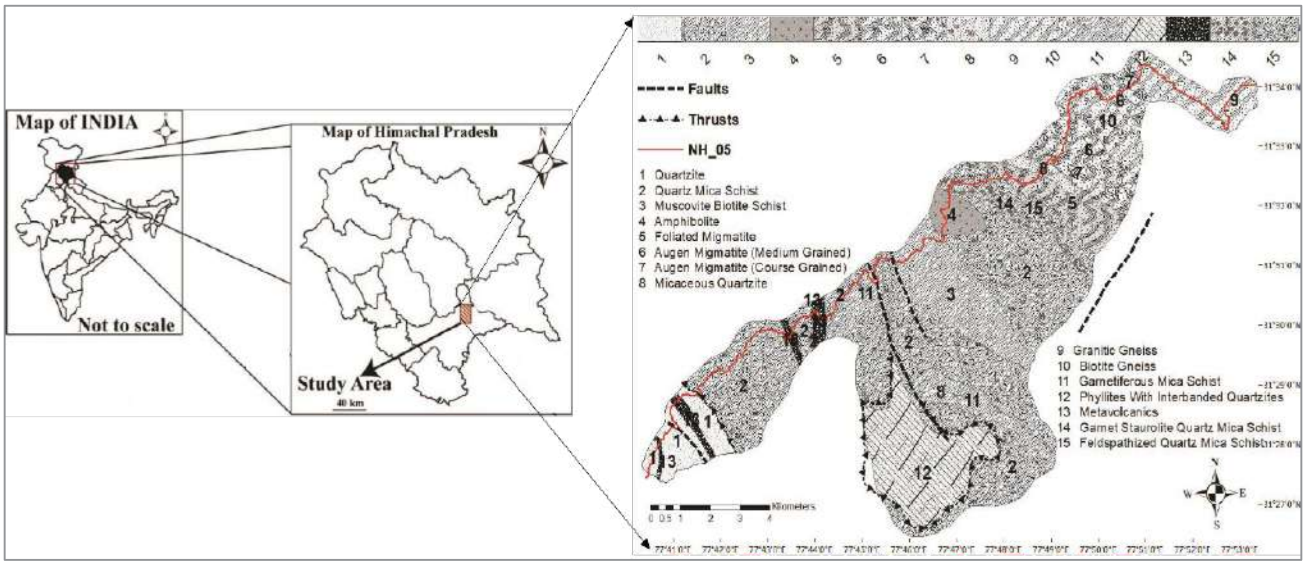

Fig. 1- Location and geological map of the study area (After Kundu et al., 2023)

Rock slope failures in highly jointed rocks regularly disturb the transportation along this strategically important NH along exposed cut slopes (Singh et al., 2021). The jointed cut slopes along the highway fail due to the complex interaction of discontinuities within the rock mass which depends upon the shear strength parameters of prevailing discontinuities coupled with their unfavourable orientation relation with the slope face (Kundu et al., 2023). The prevailing lithology in the area was classified into different rock types mainly based on mineralogy, grain size variation and colour. To collect the comprehensive roughness data and representative samples for thin section analysis, a detailed field investigation was carried out from Jhakri to Nigulsari (Fig. 2) and samples were collected for lab analysis.

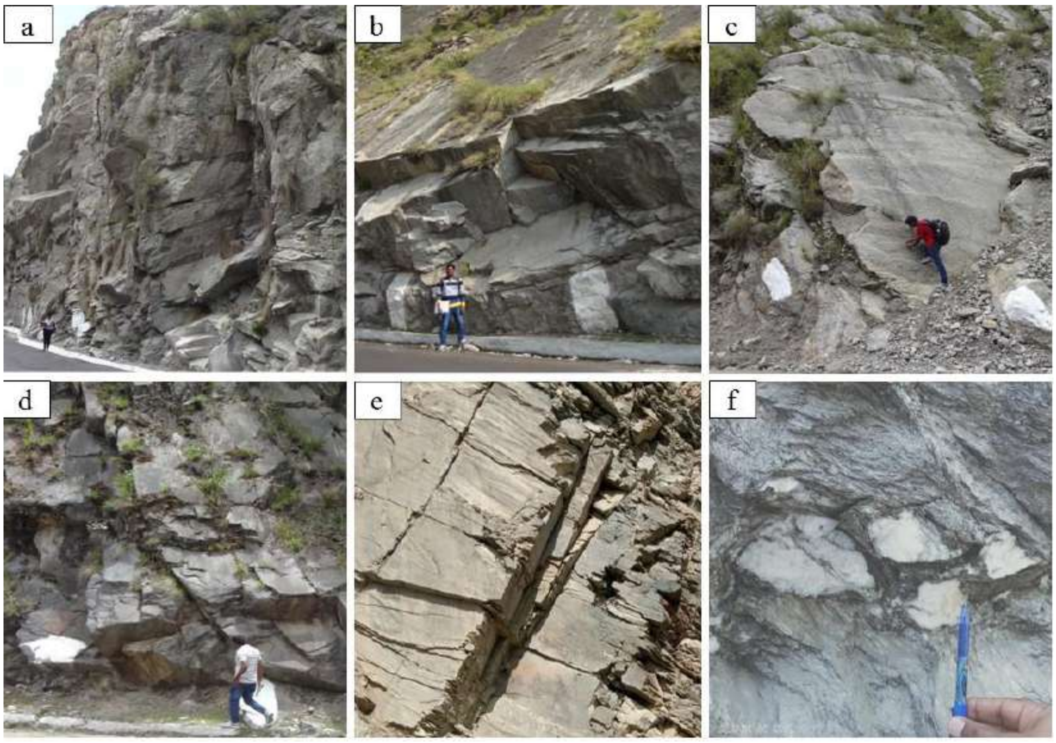

Fig. 2- Field photographs depicting different lithology and data collection along NH-5 (a) Biotite Gneiss (b) Magmatic Gneiss (c) Granitic Gneiss (d) Mica rich quartz feldspathic Gneiss (e) Mica Rich Schist and (f) Medium grained schist

3.1 Geology of Study Area

In the NW of the Himalayas, the Higher Himalaya thrusts over the Lesser Himalaya along the MCT and comprises greenschist to amphibolite facies rocks of Precambrian to Cambrian (High Himalaya Crystalline) and the Palaeozoic to Mesozoic Tethyan zone (Srikantia and Bhargava, 1998). The MCT zone consists of highly deformed mylonitic orthogenesis and Para gneisses. The study area starts near Munsiari Thrust (MT) of the Lahri-Kullu-Rampur Window (Lesser Himalaya) (Bhargava et al., 2011; Mukhopadhaya et al., 1997). The Jhakri Thrust Zone (JTZ) is one such out-of-sequence thrust in the Lesser Himalayan and is best exposed in the study area (Pandey et al., 2004). The Rampur Group consists mainly of quartzite and pene-contemporaneous volcanic/meta-volcanic rock. This area is mainly composed of mica schist with quartzite bands, pale white quartzite with phyllite bands, streaky and banded gneiss, carbonaceous slate and phyllite. The Jeori-Wangtu Banded Gneissic Complex and other Groups namely Kullu and Rampur of rocks represent the Paleoproterozoic period in the State (Srikantia and Bhargava, 1998). The Jeori-Wangtu Granitoid Gneiss is strongly foliated with well-developed Augen-gneiss, mylonitic gneiss, and porphyroblastic biotite gneiss with-foliated granitoid in the central part (Fig. 1).

4. METHODOLOGY

4.1 Collection of Surface Roughness Profiles in the Field

In the field, joint roughness data for various rock types are collected using a roughness profilometer, commonly known as Barton comb having a length of 10 cm (Fig. 3). While selecting surface exposure for roughness measurement, care has been taken to distinguish natural joints from those exposed fractures induced through mechanical or blasting. The rock types whose surface roughness was collected include biotite gneiss, mica-rich quartz feldspathic (MQF) gneiss, medium-grained schist, migmatite gneiss, mica-rich schist, and granitic gneiss (Fig. 2). The rocks considered in the present study are well exposed in form of cut slopes along NH-05 from Jhakri to Nigulsari. The availability of sufficient surface exposure to collect reliable field data is the reason to consider these metamorphic rocks in the present study.

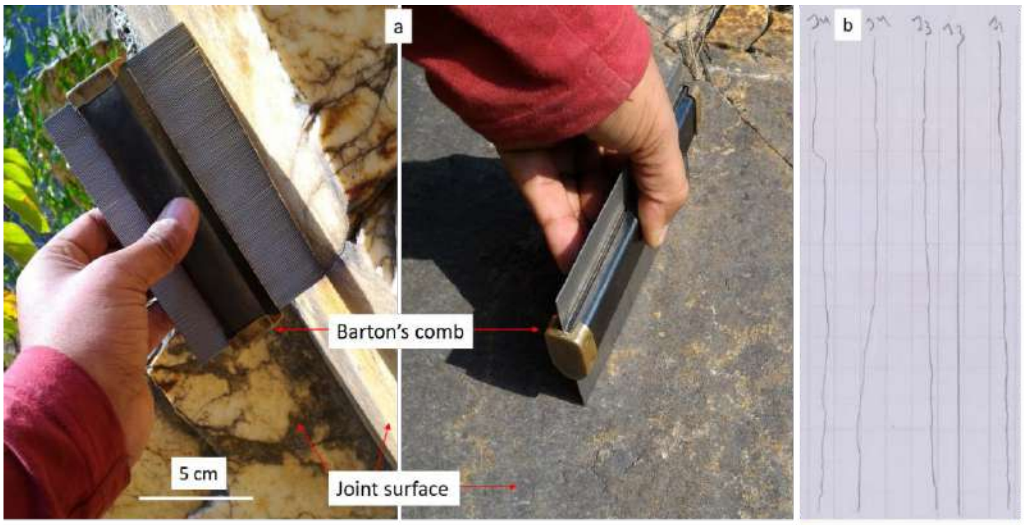

Fig. 3- (a) Assessment of joint roughness profile in the field, (b) a view of measured joint roughness profile

4.2 Profile Digitization and Estimation of Joint Roughness Coefficient

The documented roughness profiles of different joint surfaces for different rock types during the field visit were later digitized with open-source software WebPlotDigitizer, a Web-based tool to extract data points from plots, images, and maps. Before extracting the point, the recorded roughness profile was properly scaled (Fig. 4).

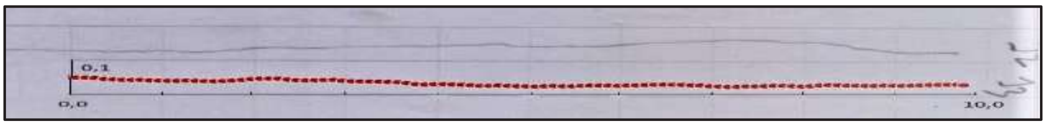

Fig. 4- Illustration of digitized scaled roughness profile of a joint surface

These digitised data sets were transformed into points with x and y coordinates. Then the points on the digitized scaled roughness profile were post-processed to obtain Z_2 (root mean square of the profile) using Equation 2;

$$Z_2 = \left[1/L \int_0^L \left(\frac{dy}{dx} \right)^2 dx \right] \tag{2}$$

where L is the total length of the profile, and (x y) is the point coordinates of the digitized profile.

As mentioned in Section 2, the correlation suggested by Tse and Cruden (1979) has been used to subsequently quantify the Joint Roughness Coefficient (JRC) using Z_2. They described the process based on Barton's standard joint profiles using the root mean square of the first derivative and suggested three empirical correlations to estimate the JRC value of a rock profile. However, based on the sampling interval between 0.5 mm to 1.27 mm, the correlation given in Equation 3 is suggested by them for JRC estimation to avoid the subjectivity involved which is a logarithmic function of Z_2. Therefore, the correlation given in Equation 3 has been considered to estimate JRC in the present study.

$$JRC = 32.2 + 32.47\log(Z_2) \qquad (3)$$

where Z_2 is the Root mean square of the first derivative.

4.2.1 Visual assessment of joint roughness

The visual judgment technique suggested in the literature (Barton & Choubey, 1977; Barton, 1973) is the conventional method for the assessment of the JRC value of the actual roughness profile compared with the standard profile (Fig. 5).

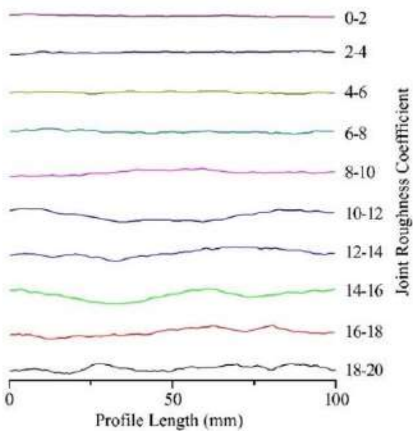

Fig. 5- Standard roughness profiles for Joint Roughness Coefficient (Barton & Choubey, 1977)

Multiple data of roughness for the same joint have been processed to avoid the chance of error in the resulted value of JRC during the data processing.

4.3 Assessment of Textural Characteristics

4.3.1 Quantitative assessment of textural parameters

Howrath & Rowland (1987) and Azzoni et al. (1996) proposed the equation for the Textural Coefficient (TC) to quantify the textural characteristics of a rock using microphotographs. The method of a quantitative assessment of rock texture consists of four components which are as follows;

- Dimension and analysis of grain circularity
- Measurement and analysis of grain elongation
- Measurement and quantification of grain orientation
- Weighting of results based upon the degree of grain packing.

Three main parameters have been suggested for the quantitative value of textural parameters which are as follows;

Form Factor (FF):

It is a measure of a grain's deviation from circularity. This deviation may occur in two ways, one is as elongation of the shape, or increased "roughness" of the grain's perimeter. For a perfect circle, the form factor should be 1. Roughness has a good correlation to the grain's form factor which is defined as;

$$\text{Form factor} = 4\pi\left[\frac{(\text{Area})}{(\text{Perimeter})^2}\right] \quad (4)$$

Grain packing weighting (AW):

It represents area weighting based on the grain packing density in any observation window as shown in Figure 6. The percentage area of grains to the total reference area is expressed as;

$$\text{AW} = \sum\left(\frac{\text{grain areas within the reference area boundary}}{\text{area boundary by the reference area boundary}}\right) \quad (5)$$

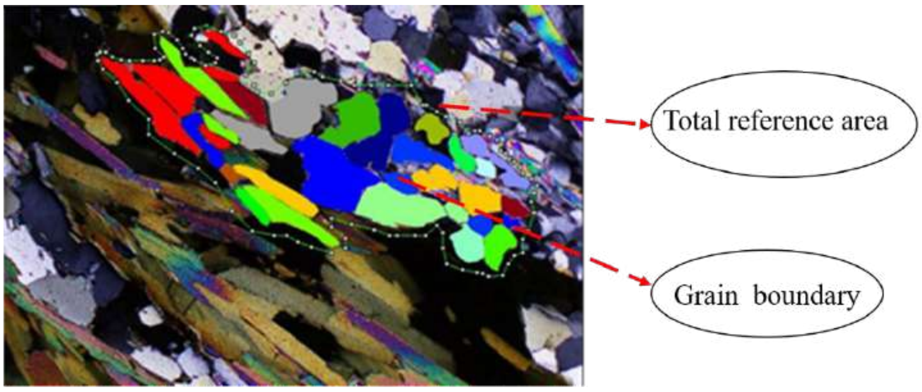

Fig. 6- Presentation of thin section outline of the total reference area and grains within the selected window in Migmatic gneiss

Angle Factor (AF):

Finally, the angle factor was calculated only for the elongated grains with an aspect ratio greater than 2. This angle factor is a quantified value of the angular orientation of grains. The parameter was calculated by a class-weighted system applied to the absolute, acute angular differences (β) vary from 0^0-90^0 between each grain. Thus, for a group of N grains, the number of unique angular differences is:

$$(N-1) + (N-2) + (N-3) + \ldots + 2+1 = (N-1)\,N/2 \quad (6)$$

The angular differences are then separated into nine classes, each of which is weighted. The classes and weightings are presented in Table 3.

Table 3- Classes and weightings for absolute, acute angular differences

No.	Class range (β)	Weighting (*i*)
1	$0 \leq 10^o$	1
2	$10 \leq \theta \leq 20$	2
3	$20 \leq \theta \leq 30$	3
4	$30 \leq \theta \leq 40$	4
5	$40 \leq \theta \leq 50$	5

6	$50 \leq \theta \leq 60$	6
7	$60 \leq \theta \leq 70$	7
8	$70 \leq \theta \leq 80$	8
9	$80 \leq \theta \leq 90$	9

Then the angle factor is calculated by summing the products of the class weightings and the fractions of the total number of angular differences in each class as follows;

$$\text{Angle Factor} = \sum_{i=1}^{9} \left(\frac{Xi}{\frac{(N-1)N}{2}} \right) * i \tag{7}$$

Where N = total number of elongated particles, X_i = number of angular differences in each class, and i = weighting factor and class number.

Textural factors such as orientation, shape, degree of grain linking, relative quantities of grains and matrix (packing density) are determined through thin section images of respective rock types using open-source software, ImageJ. The marking of the outer boundary of mineral grains in thin sections was carried out and subsequent parameters were computed.

Based on the above-mentioned textural parameters, the relation to quantify the TC is as follows;

$$TC = AW \left[\left(\frac{N_0}{N_0 + N_1} \times \frac{1}{FF_0} \right) + \left(\frac{N_1}{N_0 + N_1} \times AR_1 \times AF_1 \right) \right] \tag{8}$$

where TC = texture Coefficient; AW= grain packing weighting; N_0 = number of grains whose aspect ratio is below a pre-set discrimination level; N_1 = number of grains whose aspect ratio is above a pre-set discrimination level; FF_0= arithmetic mean of discriminated form-factors; AR_1 = arithmetic mean of discriminated aspect ratios; AF_1 = angle factor, quantifying grain orientation.

The individual analysis involved choosing an "observation window" or reference area made up of twenty to fifty rock grains and then processing the image to determine each grain's area, perimeter, length, width, and angle. The long axis and short axis of each grain of the observation window were used to determine the preset discrimination level. Since the majority of grains having long and short axis approximated by 2, therefore, the preset level was decided to be set as 2 for the discrimination of mineral grains in this study. Measurement and analysis of grain circularity are a form factor for the mineral grains that required a preset value less than 2, whereas the angle factor for the grains was calculated with a preset level higher than 2. The obtained results are presented and discussed in the next section.

5. RESULTS AND DISCUSSION

5.1 Quantification of Joint Roughness Coefficient

To quantify the roughness, the arithmetic mean of the square of the digitized data set was calculated and JRC estimation of the joint roughness profile was carried out. Thus, initially the root mean square of the first derivative of the profile i.e., Z_2 were determined for each joint profile using Equation 2. Then subsequently the JRC was calculated using Equation 3 to evaluate the performance of the given relation and their relative variations with JRC measured in the field (Table 4) are shown in Figure 7. The JRC values for the respective rock type suggest minimum ranges of 2.49 to 7.33 for Mica-rich schist. While the maximum JRC ranges from 12.54 to 13.20 for Migmatic Gneiss. The visual comparison of comb profile of the collected joint with the standard profile given by Barton and

Choubey (1977) suggested higher JRC values assigned to each profile in comparison to the quantified JRC using Z_2. Also, the difference in the value might be higher due to involved subjectivity depending on the experience of the practitioner.

Table 4- Results of calculated Z_2 and respective JRC of joint profiles for each rock type along with field JRC

Sample IDs	Rock Types	Z_2	Calculated JRC JRC=32.2+32.47 log (Z_2)	Visually measured JRC in field
1	Biotite Gneiss	0.219	10.76	12
		0.229	11.43	12
		0.219	10.76	12
2	Migmatic Gneiss	0.260	13.20	14
		0.248	12.54	14
3	Granitic Gneiss	0.232	11.60	12
		0.227	11.28	12
4	MQF Gneiss	0.199	9.42	11
5	Augen Gneiss	0.235	11.78	12
6	Mica rich schist	0.122	2.49	5
		0.171	7.33	6
		0.146	5.08	6
7	Medium-grained schist	0.199	9.42	10
		0.197	9.26	8

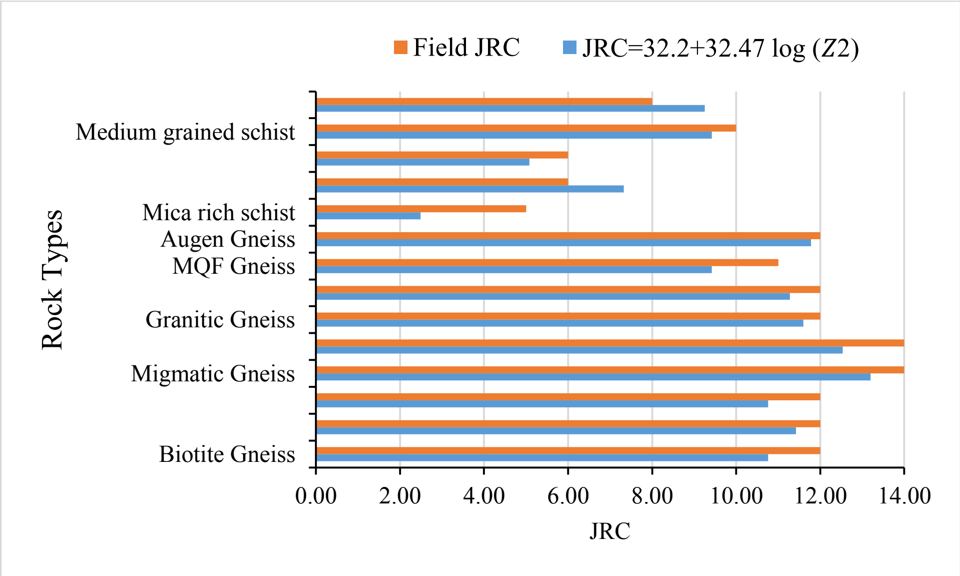

Fig. 7- Comparison of JRC values quantified through Z2 and field-measured JRC for each rock type

Regression analysis between Z_2 and its corresponding quantified JRC has been performed to check the correlation between these two variables for different roughness profiles (Fig. 8a). The result of regression analysis indicates a strong linear correlation between Z_2 and JRC with the coefficient of regression (R^2) of 0.98. The visually assessed JRC with standard profile correlated with the Z_2 depicting data scattering along the trend line with R^2 of 0.91. The correlation analysis suggests that the joint roughness coefficient can be well predicted by Equation 9 measuring Z_2 at an interval of less than 1 mm. The authors are not recommending the correlation found with visually assessed JRC due to the subjectively involved in assigning the numeric value of JRC in the field.

$$JRC = 76.33 \times Z_2 - 6.09 \quad (9)$$

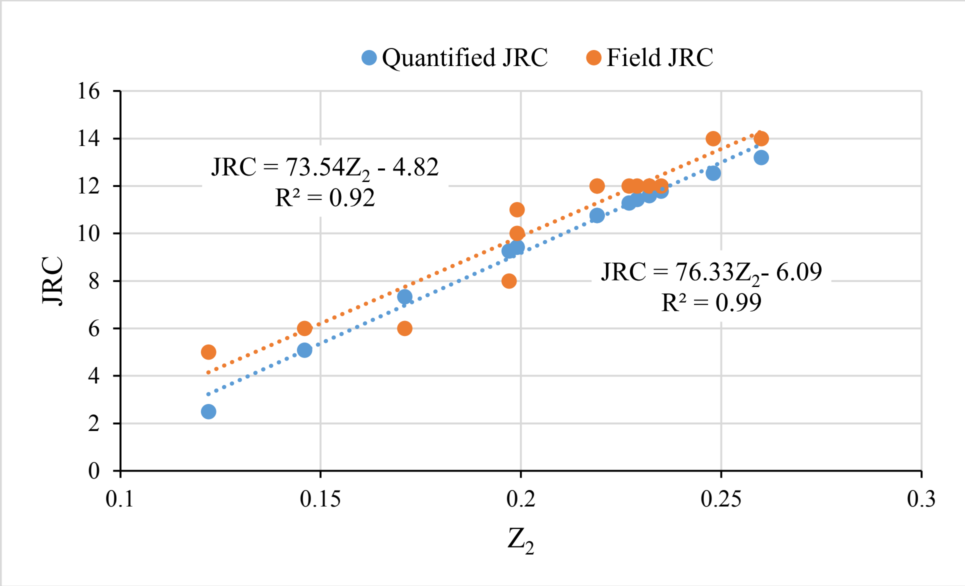

Fig. 8a- Regression analysis between Z_2 and corresponding quantified JRC as well as Field JRC

The quantified JRC using Z_2 and field measured JRC using comb profiler have also been correlated along the 1:1 line (Fig. 8b) which suggests that the higher values correspond to the field JRC and are visually overestimated.

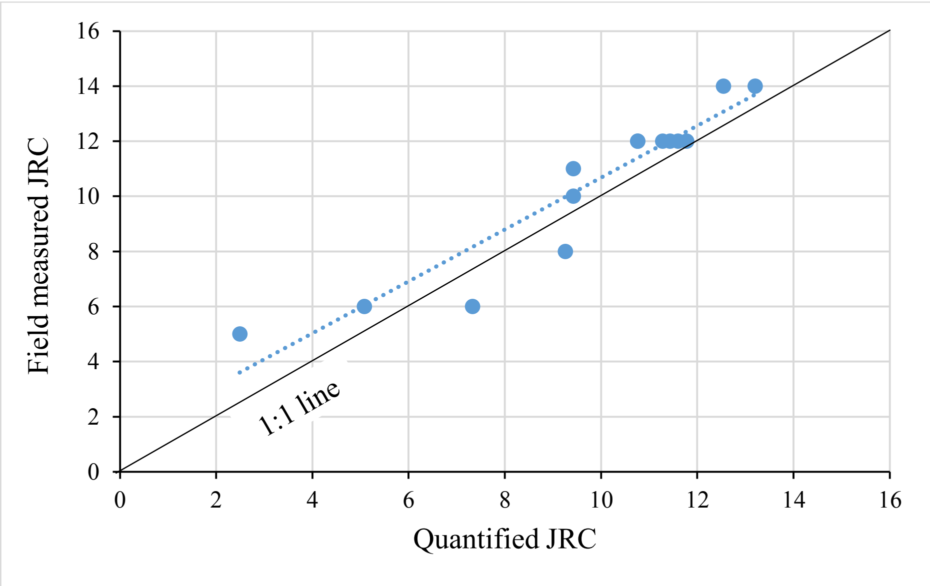

Fig. 8b- Correlation between quantified JRC and field JRC on 1:1 line

5.2 Assessment of Textural Coefficient

The TC for each rock type is calculated using the methods and procedure described in preceding Section 4.3. The major and minor minerals identified during petrographic analysis are shown in the respective thin section images (Fig. 9). The main objective here is to compute the textural characteristics for each rock type. Therefore, the processed and computed textural parameters for TC calculation for each rock type are shown in Table 5. The estimated results suggest variation in TC ranged from minimum of 0.625 for Medium-grained schist to maximum of 1.365 for Granitic gneiss.

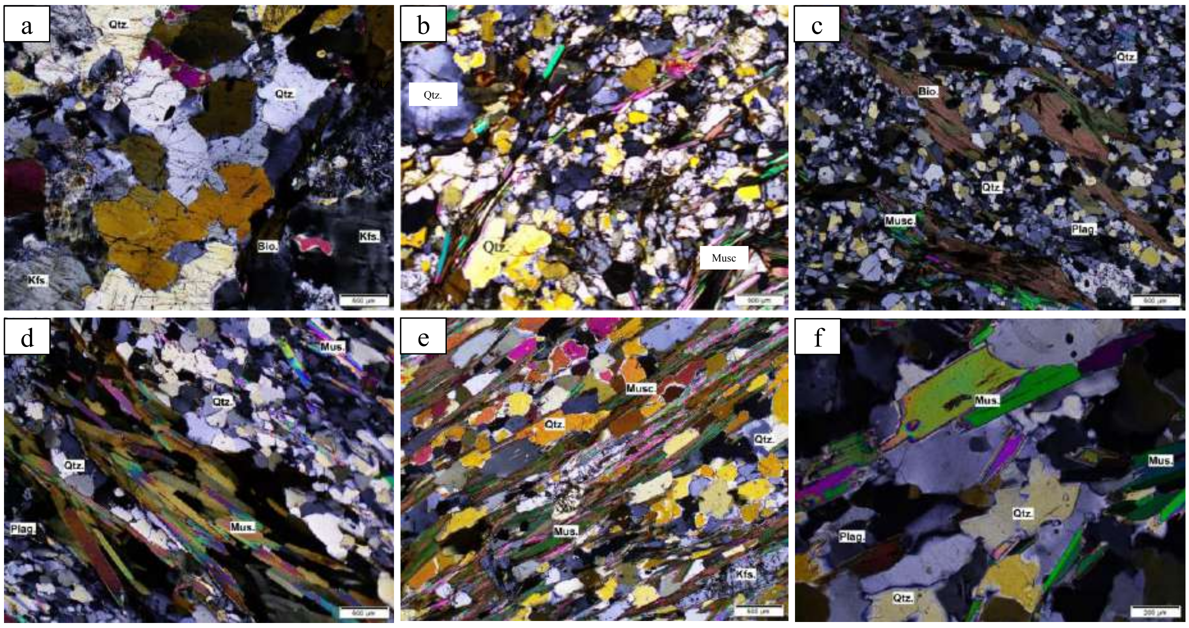

Fig. 9 Microphotographs of studied rock types (a) Biotite gneiss (b) Migmatic gneiss (c) Granitic gneiss (d) MQF gneiss (e) Mica rich schist and (f) Medium-grained schist.

Table 5- Textural parameters obtained from petrographic analyses

Sample IDs	Rock Types	AW	$N1/(N_0+N_1)$	$No/(N_0+N_1)$	$1/FF_0$	AR_1	AF_1	TC
1	Biotite Gneiss	0.712	0.556	0.444	1.667	1.521	0.65	0.919
		0.822	0.292	0.708	1.806	1.482	0.75	1.318
		0.772	0.286	0.714	1.912	1.557	0.72	1.301
2	Migmatic Gneiss	0.752	0.714	0.286	1.863	1.502	0.86	1.094
		0.891	0.571	0.429	2.115	1.578	0.67	1.345
3	Granitic Gneiss	0.752	0.364	0.636	2.250	1.530	0.69	1.365
		0.709	0.721	0.279	2.305	1.541	0.73	1.031
4	MQF Gneiss	0.694	0.217	0.783	1.885	1.519	0.84	1.215
5	Augen Gneiss	0.745	0.266	0.714	2.096	1.538	0.71	1.330
6	Mica rich schist	0.667	0.408	0.592	2.255	1.727	0.43	1.093
		0.722	0.734	0.312	1.863	1.712	0.840	1.181
		0.815	0.292	0.708	1.563	1.492	0.740	1.165
7	Medium grained schist	0.501	0.393	0.607	1.794	1.378	0.5	0.682
		0.603	0.656	0.344	1.659	1.546	0.46	0.625

5.3 Correlation between JRC and Textural Coefficient

This section explores the potential relationships between JRC and TC based on the obtained results in the preceding sections. The estimated JRC and TC for respective rock types are presented in Tables 4 and 5 respectively. The statistical models have been developed by regression analyses to establish the correlation between JRC and TC. The best-fitting curves of data points have been found by applying the least square methods.

Firstly, the correlation between TC and JRC was calculated using Equation 3 performed through regression analyses as shown in Figure 10a. Then the correlation between TC and field-measured JRC has also been plotted to check the dependency of these two variables (Fig. 10b). The regression analyses suggest two groups of data clustering, Group A and B, based on the linear best-fitting of data points in each case (Fig. 10a, b). By applying the least square method, high correlation coefficients are obtained for both groups in each case (Table 6). Group A represents the lithologies such as Augen gneiss and Mica rich schist whereas Group B consists of MQF Gneiss and Medium grained schist. However, some rock types such as Biotite gneiss, Migmatic gneiss and Granitic gneiss are common in both groups due to nonconformity in grain parameters such as grain sizes, shape and angularity etc. Based on the R^2 which measures the goodness of fit for linear regression models varied from 0.91 to 0.94 in the case of JRC obtained using Z_2 method. It signifies that the proposed correlation is very much acceptable (Fig. 10a). The TC correlation with field-measured JRC also suggests similar regression statistics, however, comparatively lower R^2 for both the Groups due to involved subjectivity during profile visualization which may vary person to person (Fig. 10b).

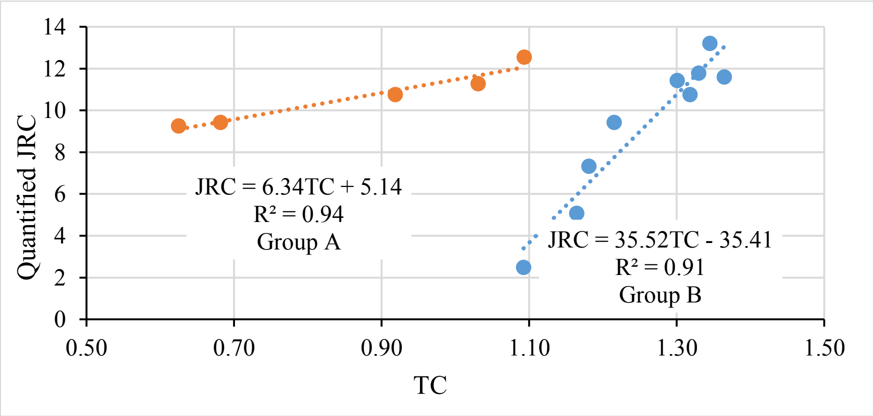

Fig. 10a- Correlation of TC with JRC calculated using Equation 3

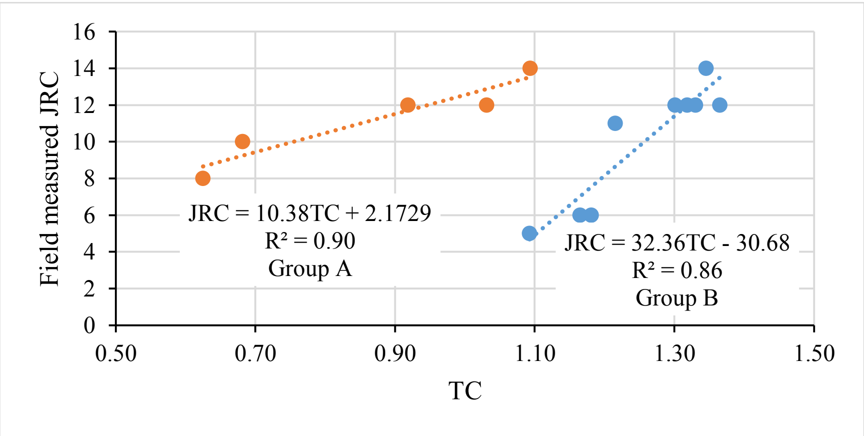

Fig. 10b- Correlation of TC with field measured JRC using comb profiler

The regression plots also signify the threshold TC limit of 1.1, based on which Group A and B are formulated. The JRC data corresponding to $TC \leq 1.1$ belongs to Group A, whereas Group B fits with the data points of JRC corresponding to $TC \geq 1.1$. Based on the observations, Group B is characterized by wide variation in JRC having less scattering in TC. Conversely, Group A has wide data scattering in TC but the difference in JRC is quite low as compared to group B. That signifies the inter-dependency of both variables and also indicates that the JRC is controlled by intrinsic textural characteristics of the rock. It is to note that the grouping of studied rocks has been done on the textural parameters and their relationship with JRC measured by Z_2 method. So, the cut-off value of TC may vary for other rock types. Also, the scale effect on JRC is not considered in the present study which has a profound influence on the shear strength characteristics of rock masses. It is well known that the JRC value reduces after introducing the scale correction factor (Barton and Bandis, 1982). Thus, considering this fact, the proposed relation with TC may change while considering the scaled JRC for a given rock type. To check the relation of TC with the proposed correlation (Eq. 9) for JRC quantification, a regression graph has also been plotted (Fig. 11) which suggests identical clustering of data points within two groups with R^2 of 0.92 in each case. The threshold TC limit of 1.1 is found as a cut-off value for Group A and B in each case which is possibly controlled by the Aspect ratio (AR) of the mineral grains as AR is positively correlated with the JRC as compared to the other textural parameters.

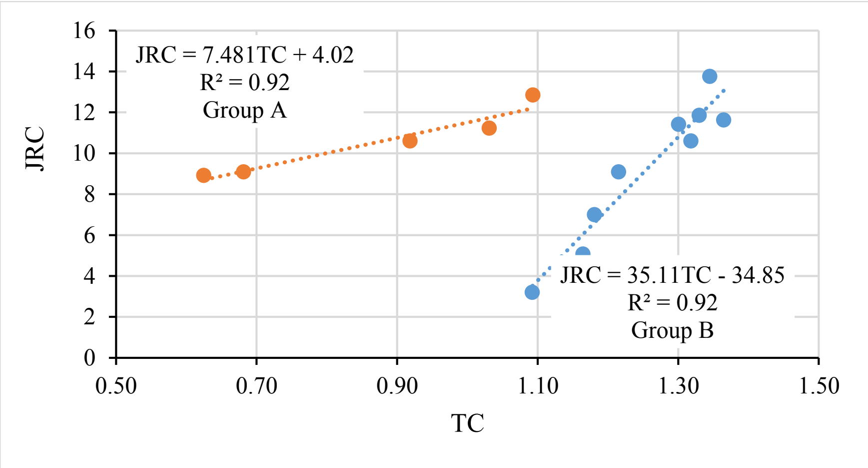

Fig. 11- Correlation of TC with JRC calculated Equation 9

As a key outcome of this study, correlation equations have been proposed particularly for Himalayan Gneissic and Schistose rocks to quantify JRC from TC and vice-versa (Table 6). One can quantify the inherent textural characteristics using these correlations by JRC measurement. Conversely, the joint roughness coefficient can be quantified using TC values applying limiting TC conditions. The proposed correlations perform well when JRC estimation is done using Z_2 method.

Table 6- Proposed empirical correlations between JRC and TC for Gneissic and Schistose rock

Methods of JRC calculation	Conditions	Proposed Correlations	R^2
$JRC=32.2+32.47\log(Z_2)$ (Tse & Cruden, 1979)	A (when TC <1.1)	JRC = 6.34×TC + 5.14	0.94
	B (when TC >1.1)	JRC = 35.52×TC - 35.41	0.91
$JRC=76.33\times Z_2-6.09$ (This study)	A (when TC <1.1)	JRC = 7.48×TC + 4.02	0.92
	B (when TC >1.1)	JRC = 35.11×TC – 34.85	0.92

6. CONCLUSIONS

Quantitative and precise estimation of joint roughness has vital importance in rock engineering projects. Considering the joint roughness dependency on textural characteristics, the present study explores the potential relation between the joint roughness coefficient and textural coefficient of the

Himalayan Gneissic and Schistose rocks. To quantify the joint roughness coefficient, root mean square of the first derivative of the joint surface profile (Z_2) has been utilized. The following concluding remarks are drawn from the present study:

- The quantified JRC using logarithmic of Z_2 yields lower JRC in most of the cases as compared to the field-measured JRC, whereas the proposed linear correlation in the present study to quantify the JRC using Z_2 exhibits higher accuracy.
- Two groups of data clustering, Group A and B (Figs. 10 & 11), are observed with a threshold TC limit of 1.1 based on the regression analyses between JRC and TC.
- The rock types having TC $\geq$ 1.1 are characterized by wide variation in roughness with less scattering in textural parameters, whereas rock types having wide scattering in TC show less variation in roughness. That signifies the control of inherent textural properties on surface waviness and its reflection on roughness quantification.
- The Z_2 method of estimating JRC is found to be more reliable as compared to TC due to direct estimation from the joint surface profile. Nevertheless, upon inaccessibility of Z_2, the proposed relation using TC can be a handy approach to quantify JRC.

Acknowledgements

First author thankfully acknowledges the support by the MHRD fellowship for PhD granted by the Indian Institute of Technology, Roorkee, India.

References

Abolfazli, M. and Fahimifar, A. (2020). An investigation on the correlation between the joint roughness coefficient (JRC) and joint roughness parameters. Construction and Building Materials; 259. https://doi.org/10.1016/j.conbuildmat.2020.120415

Azzoni, A., Bailo, F., Rondena, E., Zaninetti, A. (1996). Assessment of texture coefficient for different rock types and correlation with uniaxial compressive strength and rock weathering. Rock Mech Rock Eng.; 29:36–46

Bae, D., Kim, K., Koh, Y., Kim, J. (2011). Characterization of joint roughness in granite by applying the scan circle technique to images from a borehole televiewer, Rock Mech. Rock Eng.; 44:497–504.

Baker, B.R., Gessner, K., Holden, E., Squelch, A. (2008). Automatic detection of anisotropic, features on rock surfaces. Geosphere; 4(2): 418-428.

Bandis, S., Lumsden, A., Barton, N. (1981). Experimental studies of scale effects on the shear behaviour of rock joints. Int. J. Rock Mech. Min. Sci. Geomech. Abstr.; 18(1): 1–21.

Barton, N. (1971). A relationship between joint roughness and joint shear strength. In Rock Fracture-Proc. Int. Symp. On Rock Mechanics, Nancy, France. pp. 1-8.

Barton, N. (2013). Shear strength criteria for rock, rock joints, Rock fill and rock masses: Problems and some solutions. J. Rock Mech. Geotech. Eng.; 5(4): 249–261.

Barton, N. and Choubey, V. (1977). Shear strength of rock joints in theory and practice. Rock Mechanics and Rock Engineering; 10:1–54.

Barton, N. and de Quadros, E.F. (1997). Joint aperture and roughness in the prediction of flow and groutability of rock masses. Int J Rock Mech Min Sci.; 34: 3–4.

Barton, N. (1973). Review of a new shear-strength criterion for rock joints. Engineering Geology; 7:287–332.

Barton, N., Bandis, S., Bakhtar, K. (1985). Strength, deformation and conductivity coupling of rock joints. Int. J. Rock Mech. Min. Sci. Geomech. Abstr.; 22(3): 121–140.

Barton, N., Lien, R., Lunde, J. (1974). Engineering classification of rock masses for the design of tunnel support. Rock Mechanics; 6: 189–236.

Bhargava, O.N., Kaur, G., Deb, M.A. (2011). Paleoproterozoic paleosol horizon in the Lesser Himalaya and its regional implications. J. Asian Earth Sci.; 42:1371–1380.

Bhasin, R. and Hoeg, K. (1998). Parametric study for a large cavern in jointed rock using a distinct element model (UDEC-BB). Int J. Rock Mech Min Sci.; 35: 17–29.

Goodman, R.E., & Shi, G.H. (1985). Block theory and its application to rock engineering; Englewood Cliffs, NJ: Prentice-Hall.

Gupta, K., Satyam, N., & Gupta, V. (2023). Probabilistic physical modelling and prediction of regional seismic landslide hazard in Uttarakhand state (India). Landslides; 1-12.

Howrath, D.H., and Rowlands, J.C. (1987). Quantitative assessment of rock texture and correlation with drillability and strength properties. Rock mechanics and rock engineering; 20:57-85.

ISRM (1978). Suggested methods for the quantitative description of discontinuities in rock masses. International Society for Rock Mechanics, Commission on Standardization of Laboratory and Field Tests. Int. J. Rock Mech. Min. Sci. Geomech. Abstract. 15: 319–368

Kabeya, K.K. and Legge, T.F.H. (1997). Relationship between grain size and some surface roughness parameters of rock joints. Int. J. Rock Mech. & Min. Sci.; 34: 3-4.

Kulatilake, P.H.S.W., Um, J., Pan, G. (1997). Requirements for accurate estimation of fractal parameters for self-affine roughness profiles using the line scaling method, Rock Mech. Rock Eng.; 30:181–206

Kundu, J., Sarkar, K., Ghaderpour, E., Scarascia Mugnozza, G., Mazzanti, P. (2023). A GIS-Based Kinematic Analysis for Jointed Rock Slope Stability: An Application to Himalayan Slopes. Land; 12(2): 402.

Li, Y. and Huang, R. (2015). Relationship between joint roughness coefficient and fractal dimension of rock fracture surfaces, Int. J. Rock Mech. Min. Sci.; 75:15–22.

Li, Y. and Zhang, Y. (2015). Quantitative estimation of joint roughness coefficient using statistical Parameters. Int J Rock Mech Min Sci.; 77: 27–35.

Maerz, N., Franklin, J., Bennett, C. (1990). Joint roughness measurement using shadow profilometry, Int. J. Rock Mech. Min. Sci.; 27: 329–343.

Mukhopadhaya, D.K., Ghosh, T.K., Bhadra, B.K., Srivastava, D.C. (1997). Structural and metamorphic evolution of the rocks of the Jutogh Group, Chur half-klippe, Himachal Himalayas: A summary and comparison with the Simla area. Proc. Indian Acad. Sci.-Earth Planet. Sci.; 106; pp. 197–207.

Pandey, A.K., Sachan, H.K., Virdi, N.S. (2004). Exhumation history of a shear zone constrained by microstructural and fluid inclusion techniques: An example from the Satluj valley, NW Himalaya, Indian. J. Asian Earth Sci.; 23: 391–406

Patton, F.D. (1966). Multiple modes of shear failure in rock. 1st Congress of Int. Soc. Rock. Mech.; Lisbon, Vol. 1, pp. 509–513.

Prasad, V.V.R., Dwivedi, R.D., Swarup, A. (2013). Determination of support pressure for tunnels and caverns using block theory. Tunn Undergr Space Technol.; 37: 55–61.

Rahman, Z., Slob, S. and Hack, R. (2006). Deriving roughness characteristics of rock mass discontinuities from terrestrial laser scan data, IAEG; pp. 437.

Schneider, H.J. (1976). The friction and deformation behaviour of rock joints. Rock Mech Rock Eng.; 8: 169–184.

Singh, A.K., Kundu, J., Sarkar, K., Verma, H.K., Singh, P.K. (2021). Impact of Rock Block Characteristics on rockfall hazard and its Implications for rockfall protection Strategies along Himalayan Highways: a Case Study. Bull. Eng. Geol. Environ.; 80(7): 5347–5368.

Srikantia, S.V. and Bhargava, O.N. (1998). Geology of Himachal Pradesh; Geological Society of India; Bangalore, India. pp. 1–408.

Tatone, B.S.A. and Grasselli, G. (2010). A new 2D discontinuity roughness parameter and its correlation with JRC. Int J Rock Mech Min Sci.; 47: 1391–400.

Tatone, B.S.A., Grasselli, G. (2013). An investigation of discontinuity roughness scale dependency using high-resolution surface measurements, Rock Mech. Rock Eng.; 46(4): 657–681

Tse, R. and Cruden, D.M. (1979). Estimating joint roughness coefficients. Int J Rock Mech Min Sci.; 16(5): 303–307.

Wang, L., Wang, C., Khoshnevisan, S., Ge, Y., & Sun, Z. (2017). Determination of two-dimensional joint roughness coefficient using support vector regression and factor analysis. Engineering Geology; 231: 238-251.

Wang, Q. (1982). Study on determination of rock joint roughness by using elongation rate R. In: Proceedings of the undergoing constructions; Jinchuan, China. pp. 343–348.

Yang, Z.Y., Lo, S.C., Di, C.C. (2001). Reassessing the joint roughness coefficient (JRC) estimation using Z2. Rock Mech Rock Eng.; 34: 243–51.

Yu, X.B. and Vayssade, B. (1991). Joint profiles and their roughness parameters. Int. J. Rock Mech. Min. Sci. Geomech. Abstr.; 28: 333–336.